Optimal Tuning of Tokamak Plasma Equilibrium Controllers in the Presence of Time Delays

Eugenio Schuster, David Sondak, Reza Arastoo, Michael L. Walker and David A. Humphreys

***Abstract*— When designing the control loops for tokamaks, it is important to acknowledge the effects of time delays. An assumption sometimes made for tokamaks having superconducting coils is that these extra time delays will not have any undesirable effects on control. In fact, introducing extra delays into the axisymmetric control loops of certain superconducting tokamaks can have significant detrimental consequences. Aside from qualitative observations, the detrimental effects of extra time delays in tokamak control loops are not always well understood outside the control community. This study exposes and quantifies the detrimental effects imposed by time delays in the control loop in superconducting tokamaks, by focusing on plasma current control and radial position control in a vertically stable circular plasma in the KSTAR tokamak. Delays in the power supplies, data acquisition, and vessel structure are taken into account. Extremum-seeking-based optimal tuning of PID controllers is proposed as a possible method for remediating the negative effects of time delays. The Nyquist dual locus technique is employed to assess stability of the optimally tuned closed-loop system in the presence of time delays.**

I. Introduction

With the introduction of fully superconducting tokamaks comes the need to understand how to operate and control plasmas within these devices, given new constraints imposed by superconducting PF coils. There is a concern about AC losses triggering coil quench. The minimum distance of coils from the plasma is increased due to cryogenic insulation requirements. There is a greater emphasis on minimizing the number of control coils due to cost. Passive structures are often more conductive, due to requirements for increased structural strength, multiple conducting walls, or intentional placement of highly conductive passive conductors near the plasma to reduce the growth rate of instabilities.

All of these changes from present devices tend to change the plasma shape control properties, several of them negatively because of increased delays in responding to plasma disturbances. One response to worries about AC losses is to impose limits on the speed of response of the coils. (Contrary to sometimes-stated opinion, the natural response of superconducting coils are not intrinsically slower than conductive coils of the same cross-section and number of turns, since the relevant response time is determined by the coil inductance, which is defined purely by coil geometry.) Larger distances between coils and plasma mean larger changes in coil currents are needed to accomplish the same change in shape-controlling magnetic field at the plasma. Fewer control coils means fewer controllable degrees of freedom, or conversely, less redundancy in controlling the most critical degrees of freedom. Increased conductivity in passive structures implies longer delays in magnetic field penetrating these structures and affecting the plasma.

This work was supported in part by the NSF CAREER award program (ECCS-0645086), and DoE contract number DE-FC02-04ER54698. E. Schuster (schuster@lehigh.edu), D. Sondak and R. Arastoo are with the Department of Mechanical Engineering and Mechanics, Lehigh University, Bethlehem, PA 18015, USA. M. L. Walker and D. A. Humphreys are with the DIII-D tokamak, General Atomics, San Diego, California, USA.

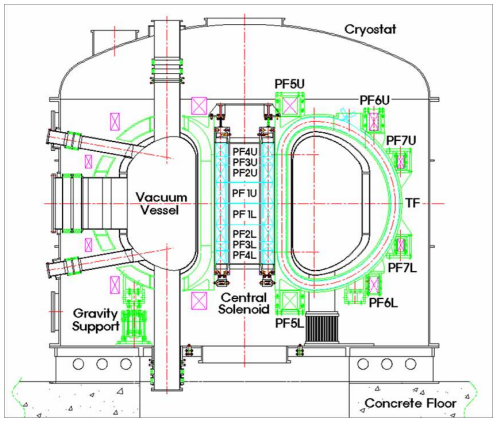

Fig. 1. KSTAR tokamak.

It is sometimes assumed in the fusion community that, because superconducting tokamaks already have significant intrinsic or imposed sources of control delay, introducing extra delays into the axisymmetric control loops will have negligible detrimental impact on the plasma control. Since it is not obvious what constitutes an acceptable amount of delay, we have begun a study of this issue in an attempt to provide guidance to designers of external systems (primarily power supplies, control computers, and communication networks) regarding acceptable pure delays (and also phase lags) contributed by these systems. This study has been carried out using models of the KSTAR (Korea Superconducting Tokamak Advanced Research) tokamak, which has recently begun operation in Daejon, Korea [1]. A cross-section of the KSTAR Tokamak is shown in Fig. 1. The active control coils outside of the vacuum vessel are superconducting and are used to establish the plasma equilibrium.

In this work we consider a vertically stable circular plasma. Two PID controllers are proposed for plasma current and radial position control. Extremum seeking [2] is proposed for optimal tuning of the PID gains in presence of time delays. Extremum seeking, which is a nonmodel-based method, iteratively modifies the arguments of a cost function (in this application, the PID parameters) so that the tracking error is minimized [3] (see references therein for alternative PID tuning methods). The stability analysis of the closed-loop system is carried out using the dual-locus

diagram (also called Satche diagram) method [4], [5]. The dual-locus diagram method is an extension or a variant of the well-known Nyquist diagram, and is also based on the celebrated argument principle in complex theory. The dual-locus diagram method is simple, intuitive and quite effective in assessing stability of time-delay systems when the time delays appear in only one of the loci.

The paper is organized as follows. Section II describes the control method for plasma current and radial position regulation. Extremum seeking is briefly introduced in Section III, where in addition the method for PID tuning is described. The effects of time delays are discussed in Section IV and the effectiveness of extremum-seeking optimal PID tuning as a method to counteract these effects is illustrated in Section V. Given the optimal PID gains, the stability of the feedback loops is assessed using the dual locus method in Section VI. Conclusions and plans for future work are summarized in Section VII.

II. Methodology

The system composed of plasma, shaping coils, and passive structure can be described using circuit equations derived from Faraday's Law, and radial and vertical force balance relations for a particular plasma equilibrium. In addition, rigid radial and vertical displacement of the equilibrium current distribution is assumed, and a resistive plasma circuit equation is specified. The result is a circuit equation describing the linearized response, around a particular plasma equilibrium, of the conductor-plasma system to voltages applied to active conductors. The model equations for poloidal field (PF) coil current, vessel (passive conductor) currents, and plasma current are respectively

$$\begin{array}{rcl} M^*_{cc}\dot{I}_c + R_c I_c + M^*_{cv}\dot{I}_v + M^*_{cp}\dot{I}_p &=& V_c \\ M^*_{vv}\dot{I}_v + R_v I_v + M^*_{vc}\dot{I}_c + M^*_{vp}\dot{I}_p &=& 0 \\ M^*_{pp}\dot{I}_p + R_p I_p + M^*_{pc}\dot{I}_c + M^*_{pv}\dot{I}_v &=& V_{no} \end{array} \quad (1)$$

where I_c, I_v, and I_p represent currents in PF coils, vessel, and plasma, respectively. V_c is the vector of voltages applied to the PF coils, and V_{no} is the effective voltage applied to drive plasma current by noninductive sources. R_a, for $a \in \{c, v, p\}$, represents the resistance matrix of each one of the circuits. $M^*_{ab} = M_{ab} + X_{ab}$ are plasma-modified mutual inductance, where $a, b \in \{c, v, p\}$. M_{ab} is the usual conductor-to-conductor mutual inductance, and X_{ab} describes a plasma motion-mediated inductance, linearized around the plasma equilibrium. The plasma response matrix X_{ab}, representing changes in flux due to plasma motion, are functions only of the equilibrium current distribution $\jmath_{eq}$ and vacuum magnetic field B_{eq}. The X_{ab} matrix is computed starting with an EFIT equilibrium [6], and added to the mutual inductance M_{ab} as part of the model construction process. In contrast to the dynamic equation (1), the mapping from currents to outputs (for example, diagnostic data such as flux loops, magnetic probes, Rogowskii loops) is expressed explicitly in terms of current deviations from equilibrium values [7]:

$$\delta y = C_{I_c}\delta I_c + C_{I_v}\delta I_v + C_{I_p}\delta I_p \quad (2)$$

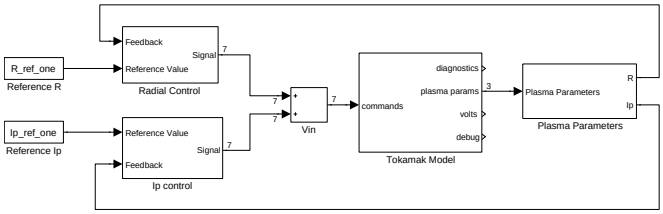

Fig. 2. The feedback loop for radial and plasma current control.

where $\delta T = T - T_{eq}$, for $T \in \{I_c, I_v, I_p, y\}$. The subscript "$eq$" denotes values at the equilibrium from which the model (1)–(2) are derived. In the rest of the paper, δ will be omitted for simplicity, but it will be implicitly assumed that the output equation is written in terms of deviation variables. The matrices C_{I_s}, for $I_s \in \{I_c, I_v, I_p\}$, are defined as

$$C_{I_s} = \frac{\partial y}{\partial I_s} + \frac{\partial y}{\partial r_c}\frac{\partial r_c}{\partial I_s} + \frac{\partial y}{\partial z_c}\frac{\partial z_c}{\partial I_s}, \quad (3)$$

where the first term on the right hand side is the "direct" response, e.g., given by Green's function calculations in the case of magnetic probes or flux loops. The remaining terms are responses due to motion of the plasma; r_c and z_c denote the radial and vertical positions of the plasma current centroid, i.e., "center of mass" of the current. It is common to include disturbance terms describing the response to variations in kinetic and current profile quantities such as poloidal beta (β_p), and normalized internal inductance (ℓ_i) [8]. However, disturbance terms are neglected in the present study.

For control design purposes, the linearized plasma response model (1)–(3) is written in state space form

$$\dot{x} = Ax + Bu, \quad y = Cx + Du \quad (4)$$

where $x = [I_c^T\ I_v^T\ I_p^T]^T$, $u = [V_c^T\ 0\ V_{no}^T]^T$. The system matrices are $A = -M^{-1}R$, $B = M^{-1}$, $C = [C_{I_c}^T\ C_{I_v}^T\ C_{I_p}^T]^T$, $D = 0$, where

$$M = \begin{bmatrix} M^*_{cc} & M^*_{cv} & M^*_{cp} \\ M^*_{vc} & M^*_{vv} & M^*_{vp} \\ M^*_{pc} & M^*_{pv} & M^*_{pp} \end{bmatrix}, \quad R = \begin{bmatrix} R_c & 0 & 0 \\ 0 & R_v & 0 \\ 0 & 0 & R_p \end{bmatrix},$$

and R is a diagonal matrix.

Figure 2 shows the feedback control architecture for control of the circular plasma. Due to the vertical stability of the circular plasma the two primary parameters of interest from a control point of view are the radial position and plasma current. Each of these parameters is controlled by its own PID controller. G^r_p and G^r_d stand for the proportional and derivative gains, respectively, of the radial position PD controller (no integral action). G^i_p and G^i_i stand for the proportional and integral gains, respectively, of the plasma current PI controller (no derivative action). The radial position of the plasma is controlled using poloidal field coil PF7 (PF7U and PF7L connected in series; see Fig. 1). The plasma current is controlled using the ohmic current vector I_{ohm} [9]. The I_{ohm} vector of poloidal field currents ideally produces zero field, or equivalently constant flux, across the plasma. This constant flux, usually referred to as ohmic flux, drives the plasma current without affecting the shape (radial

position in our case) of the original equilibrium. The concept of ohmic flux, which is common one in tokamak plasma physics, ideally decouples the plasma current and radial position control loops. Practically, some coupling always remains, but this coupling is treated as a disturbance by the "decoupled" control loops.

III. EXTREMUM SEEKING OPTIMAL CONTROL

Extremum seeking control, a popular tool in control applications in the 1940-50's, has seen a resurgence in popularity as a real time optimization tool in different fields of engineering [2]. Extremum seeking is applicable in situations where there is a nonlinearity in the control problem, and the nonlinearity has a local minimum or a maximum. The parameter space can be multidimensional. Here, we use extremum seeking for iterative optimization of the PID gains G_p^r, G_d^r, G_p^i and G_i^i (θ in Fig. 3) of the radial position PD controller and the plasma current PI controller to minimize the tracking error, i.e., to minimize the cost function

$$J = \sqrt{\int_{t_i}^{t_f} \left(\frac{R^{ref} - R}{K_R}\right)^2 + \left(\frac{I_p^{ref} - I_p}{K_I}\right)^2 dt}. \quad (5)$$

The weighted tracking error in (5) was defined so that "$1\,cm$ of error between the radial position R and its reference value R^{ref} gives the same tracking error value as $2.5\,kA$ of error between the plasma current I_p and its reference I_p^{ref}" ($K_R = .01$ and $K_{I_p} = 2500$).

We update the parameters θ (i.e., controller gains) after each simulated tokamak "discharge." Thus, we employ the discrete-time variant of extremum seeking [10]. The implementation is depicted in Figure 3, where q denotes the variable of the Z-transform. The high-pass filter is designed as $0 < h < 1$, and the modulation frequency ω is selected such that $\omega = \alpha\pi$, $0 < |\alpha| < 1$, and α is rational. The static nonlinear block $J(\theta)$ represents the tracking error of the discharge. If J has a minimum, its value is denoted by J^* and its argument by θ^*. The objective is to minimize J by driving θ to θ^*. Given the simulated plasma current I_p and radial position R evolutions for the closed-loop system in Fig. 2, the output of the nonlinear static map, $J(k) = J(\theta(k))$, for each simulated discharge k, is obtained by evaluating (5) and used to compute $\theta(k+1)$ according to the extremum seeking procedure in Fig. 3, or written equivalently as

$$\begin{aligned} J_f(k) &= -hJ_f(k-1) + J(k) - J(k-1) && (6)\\ \xi(k) &= J_f(k) b\cos(\omega k - \phi) && (7)\\ \hat{\theta}(k+1) &= \hat{\theta}(k) - \gamma\xi(k) && (8)\\ \theta(k+1) &= \hat{\theta}(k+1) + a\cos(\omega(k+1)). && (9) \end{aligned}$$

We are dealing with a multi-parameter extremum seeking procedure (4 parameters). Thus, we write

$$\theta(k) = \begin{bmatrix} \theta_1(k) \\ \theta_2(k) \\ \theta_3(k) \\ \theta_4(k) \end{bmatrix}, \ \hat{\theta}(k) = \begin{bmatrix} \hat{\theta}_1(k) \\ \hat{\theta}_2(k) \\ \hat{\theta}_3(k) \\ \hat{\theta}_4(k) \end{bmatrix}, \ \xi(k) = \begin{bmatrix} \xi_1(k) \\ \xi_2(k) \\ \xi_3(k) \\ \xi_4(k) \end{bmatrix}.$$

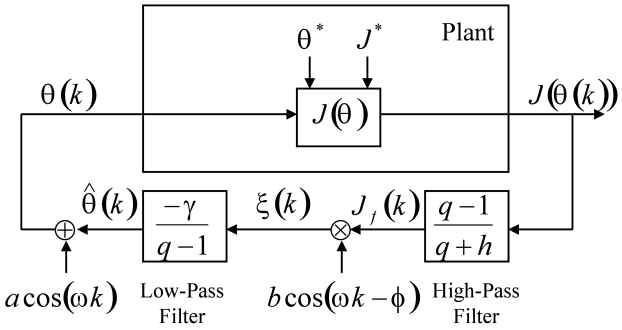

Fig. 3. Extremum seeking control scheme.

The extremum seeking constants shown in Figure 3 are written as

$$\begin{aligned} a = b &= diag\,([a_1 \quad a_2 \quad a_3 \quad a_4])\\ \gamma &= diag\,([\gamma_1 \quad \gamma_2 \quad \gamma_3 \quad \gamma_4]). \end{aligned}$$

In addition, we denote

$$\cos(\omega k) = \begin{bmatrix} \cos(\omega_1 k) \\ \cos(\omega_2 k) \\ \cos(\omega_3 k) \\ \cos(\omega_4 k) \end{bmatrix}, \ \cos(\omega k - \phi) = \begin{bmatrix} \cos(\omega_1 k - \phi_1) \\ \cos(\omega_2 k - \phi_2) \\ \cos(\omega_3 k - \phi_3) \\ \cos(\omega_4 k - \phi_4) \end{bmatrix}.$$

Fig. 4 shows the extremum seeking result for the ideal case without delay ($\tau = 0$). Fig. 4(b) shows the evolution of the cost function for 200 extremum seeking iterations. It is possible to note from Fig. 4(c) that although θ_3 (G_p^i) keeps evolving, the cost function does not vary much and reaches a practical minimum very fast in less than 20 iterations. Fig. 4(a) shows acceptable tracking performance by the controllers when tuned with the optimal gains provided by the extremum seeking optimization.

IV. TIME DELAY EFFECTS

Fig. 5 shows the effect of time delays in the Plasma Control System (PCS) when the optimal gains obtained for the ideal no-time-delay are implemented for the controllers. By introducing a delay of 1 ms into the PCS we find that the responses of the radial position and plasma current do not vary much from the no-time-delay case. However, at 3 ms, the time delay starts showing its effect on the system. With a delay of 5 ms, both responses have deteriorated. The radial position response and the plasma current response are both exhibiting a great deal of oscillation. However, both parameters are still roughly tracking the reference values on average. With a time delay of 7 ms, control is essentially lost. The plasma current response is incapable of tracking the reference value over the given time period of 1600 ms. Both responses become unstable. Studies considering phase lags in the power supplies and artificially modified vessel element resistances show similar results. Note that the magnetic field generated by the induced vessel current will oppose and have a partial canceling effect on the magnetic field generated by the poloidal field coil currents. This in turn will cause the poloidal field to have a slower effect on the plasma current. Therefore, we can consider varying vessel resistances as a parameter that causes a type of delay in the control loop.

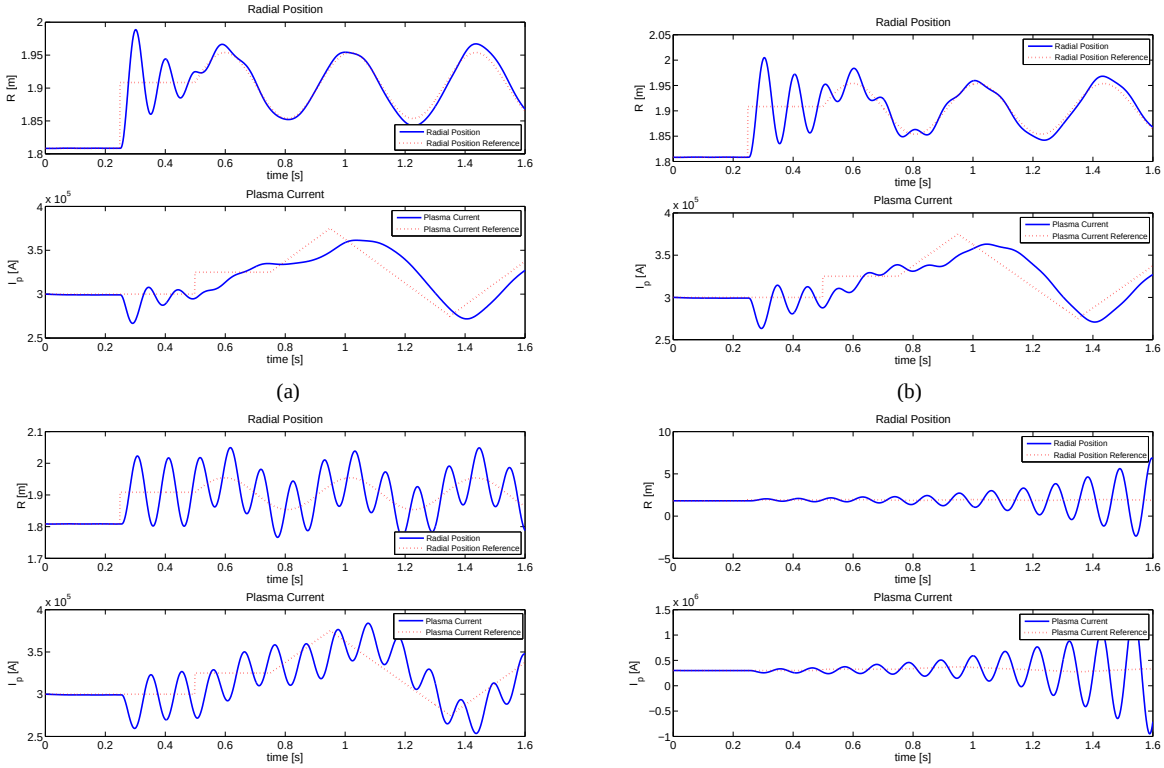

Fig. 5. Closed-loop time response with PID gains tuned by extremum seeking ($\tau = 0$): $G_p^r = 144960$, $G_d^r = 0.7384$, G_p^i = 0.0255, $G_d^i = 0.0007195$. (a) $\tau = 1$ ms, (b) $\tau = 3$ ms, (c) $\tau = 5$ ms, (d) $\tau = 7$ ms.

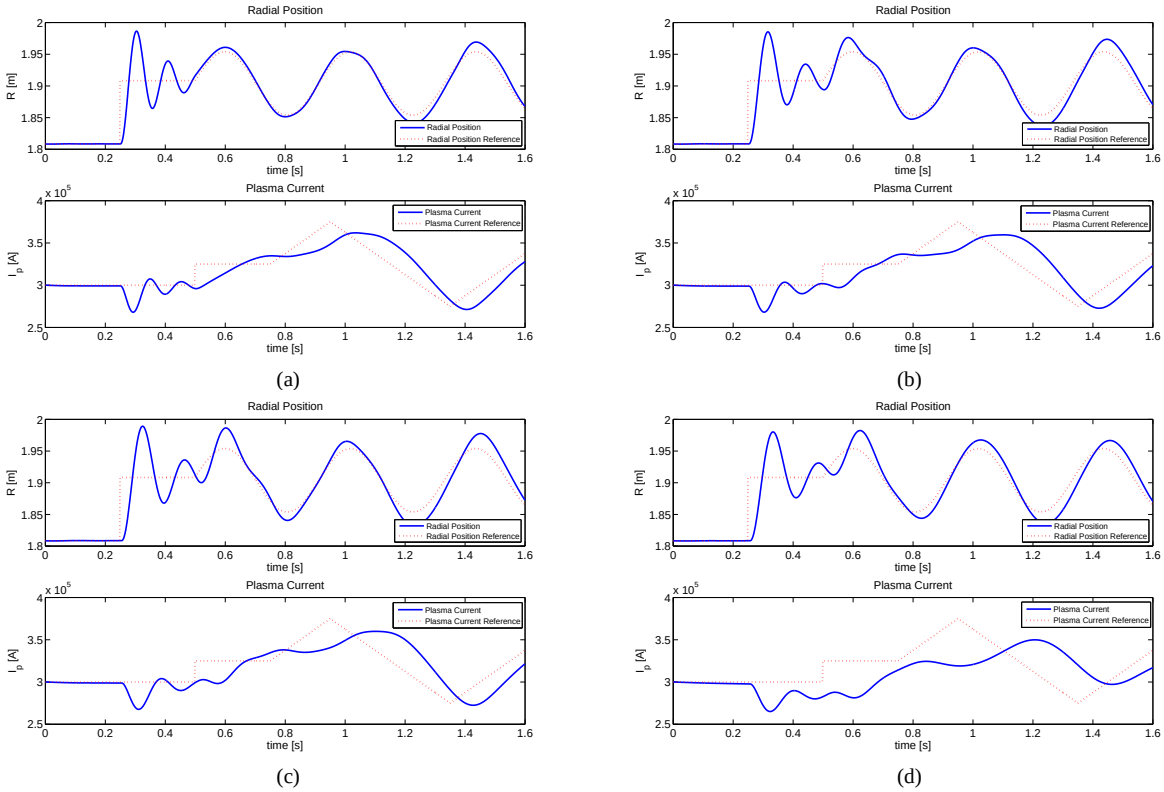

Fig. 6. Closed-loop time response with PID gains tuned by extremum seeking: (a) $\tau = 1$ ms, $G_p^r = 131635$, $G_d^r = 0.7355$, $G_p^i == 0.0264$, $G_d^i = 0.000732$, (b) $\tau = 3$ ms, $G_p^r = 96049$, $G_d^r = 0.4809$, $G_p^i = 0.0193$, $G_d^i = 0.000483$, (c) $\tau = 5$ ms, $G_p^r = 81214$, $G_d^r = 0.5154$, $G_p^i = 0.0177$, $G_d^i = 0.000603$, (d) $\tau = 7$ ms, $G_p^r = 66662$, $G_d^r = 0.0334$, $G_p^i = 0.0055$, $G_d^i = 0.000027$.

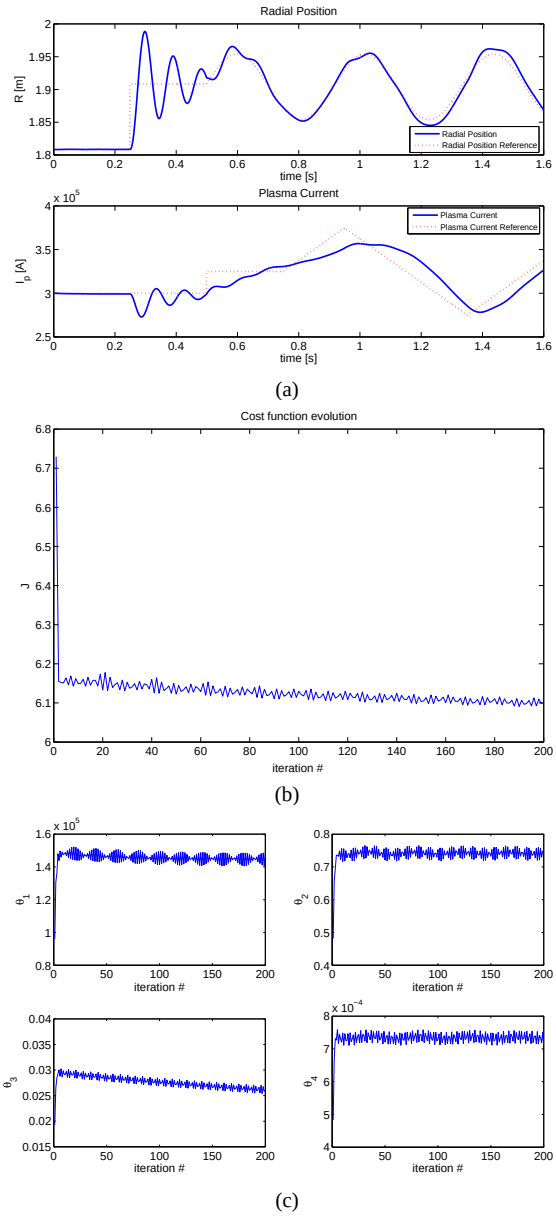

Fig. 4. PID optimal tuning by extremum seeking ($\tau = 0$): $\theta_1^* = G_p^r = 144960$, $\theta_2^* = G_d^r = 0.7384$, $\theta_3^* = G_p^i = 0.0255$, $\theta_4^* = G_i^i = 0.0007195$. (a) Time response, (b) Cost function [dB], (c) Parameters.

V. PID Optimal Tuning in Presence of Delays

The detrimental effects of time-delays in the control loops were discussed in the previous section. In order to remediate those effects the PID gains can be optimally tuned based on the estimated time delays. Fig. 6 shows the time responses of the system for the same values of time delays shown in Fig. 5. However, in these cases the PID gains were re-tuned based on the time delay present in the system instead of keeping the PID gains obtained for the ideal no-delay case. From this simulation study it is possible to conclude that extremum-seeking-based optimal tuning of PID gains arises as an effective method to cope with the time delays. In addition, and probably most importantly, it is also possible to note from both time responses (but particularly from the plasma current time response) that the tracking quality of the controllers deteriorates as the time delay increases regardless of the optimal setting of the PID gains. This implies that in terms of performance there is a practical limit of time delays that well-tuned PID controllers can handle. Fig. 7 illustrates the extremum-seeking optimization procedure for the $\tau = 1$ ms case.

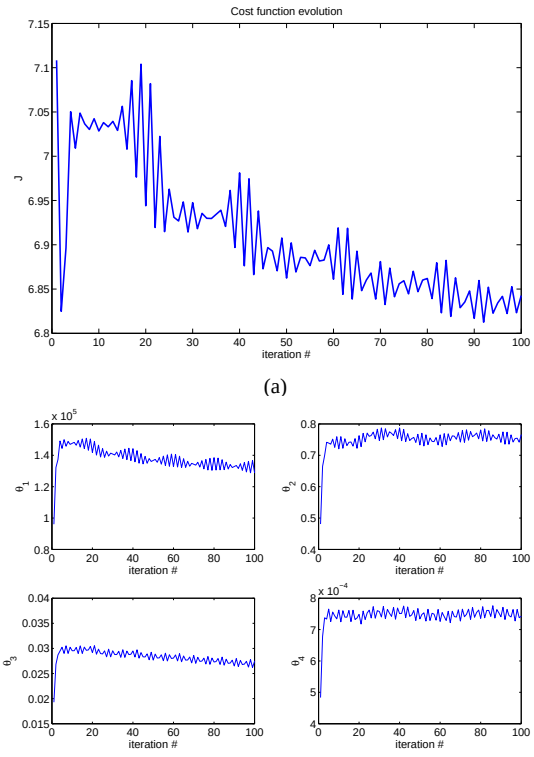

Fig. 7. PID optimal tuning by extremum seeking ($\tau = 1$ ms): $\theta_1^* = G_p^r = 131635$, $\theta_2^* = G_d^r = 0.7355$, $\theta_3^* = G_p^i = 0.0264$, $\theta_4^* = G_d^i = 0.000732$. (a) Cost function [dB], (b) Parameters.

VI. Stability Analysis of the System

To prove the stability of the time-delayed closed-loop system, we use the dual-locus method. The dual-locus technique, an extension of the Nyquist diagram technique, was proposed by Satche [4] and then developed by Smith [5].

Lemma 1: (Argument principle [11]) Suppose that a function F is meromorphic in a simply connected domain D. Suppose further that Γ_c is a Jordan curve in D, followed in the positive (anticlockwise) direction, and that F has no poles or zeros on Γ_c. If Z and P denote the number of the zeros and poles, respectively, of F in the interior of Γ_c, counted with multiplities, then the variation of the argument of $F(s)$ along the Jordan curve Γ_c is $2\pi(Z - P)$ and the winding number of $F(s)$ round the point 0, i.e. the number of times $F(s)$ winds round the origin, is $Z - P$.

Both closed-loop transfer functions of our system can be represented as

$$\frac{G(s)e^{-\tau s}}{1 + G(s)e^{-\tau s}} \tag{10}$$

where $G(s)$ is an stable transfer function. Stability of (10) has been extensively studied using different approaches

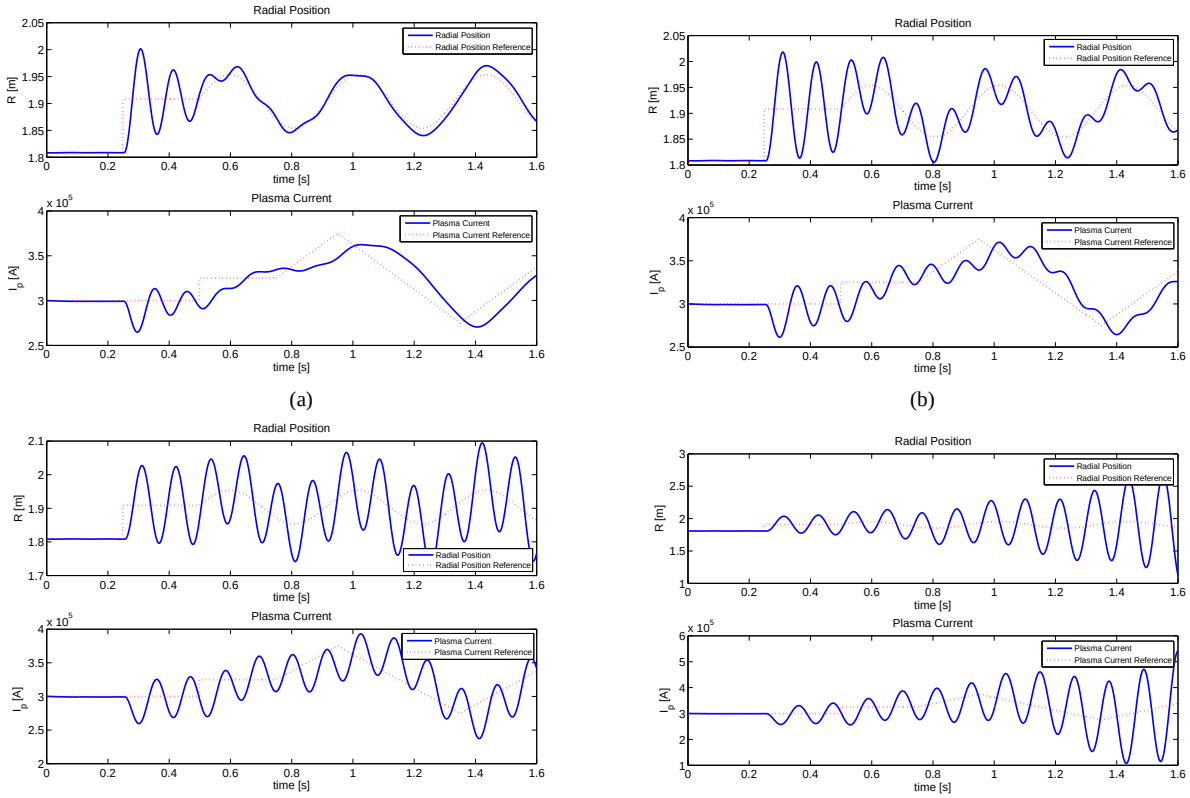

Fig. 9. Closed-loop time response with PID gains tuned by extremum seeking ($\tau = 1$ ms): $G_p^r = 131635$, $G_d^r = 0.7355$, $G_p^i == 0.0264$, $G_d^i = 0.000732$. (a) $\tau = 3$ ms, (b) $\tau = 5$ ms, (c) $\tau = 6$ ms, (d) $\tau = 7$ ms.

(see [12], [13] for instance). The characteristic equation of the closed loop system can be written as $F(s) = 0$ with $F(s) = e^{\tau s} + G(s)$. Let Γ_c be the Nyquist contour and thus enclose the entire right half of the s-plane with the exception of singularities on the imaginary axis. From the Argument principle, and since $F(s)$ has no pole in D ($G(s)$ is stable and $P = 0$), the closed-loop system is stable (i.e., $Z = 0$) if and only if the variation of the argument of $F(s) = e^{\tau s} + G(s)$ is zero.

To apply this stability criterion a plot of $F(s)$ is needed, which requires the addition of $G(s)$ and $e^{\tau s}$. To avoid the summation of these two frequency-dependent functions, we plot separately $G(s)$ and $-e^{\tau s}$ (dual-locus). The Nyquist plot of $e^{\tau s}$ is always a counterclockwise unit circle starting at the point $-1 + j0$ for $\omega = 0$. Fig. 8 shows the dual-locus for both the radial position and plasma current loops.

Noting that the characteristic equation can be rewritten as $G(s) = -e^{\tau s}$, the stability criterion can be evaluated from the dual-locus. The existence of an enclosure of the origin by $F(s)$ (or alternatively of $-e^{\tau s}$ by $G(s)$), and therefore the stability of the system, can be evaluated from the dual-locus using the difference vector and frequency distributions techniques [14]. Under the condition that $n > m$ and $\|a_m/b_n\| < 1$, where m and n denote the degrees of numerator and denominator of $G(s)$, and a_m and b_n denote the leading coefficients of the numerator and denominator, the stability criterion implies that the closed-loop is stable if one of the following conditions holds [15]:

1) The equation $\|G(j\omega)\| = 1$ has no positive real roots.
2) The equation $\|G(j\omega)\| = 1$ has one positive real root at $\omega = \omega_c$, and the inequality $-\pi + \tau\omega_c < arg[G(j\omega_c)]$ holds.
3) The equation $\|G(j\omega)\| = 1$ has two positive real roots at the frequencies ω_{c1} and ω_{c2} ($\omega_{c1} < \omega_{c2}$), and

$$-\pi + \theta\omega_{c2} < arg[G(j\omega_{c2})] \tag{11}$$

or

$$\frac{1}{\omega_{c1}} arg[G(j\omega_{c1})] + (2k+1)\pi < \theta < \frac{1}{\omega_{c2}} arg[G(j\omega_{c2})] + (2k+1)\pi \tag{12}$$

Here $k = 0, 1, 2, ..., p$,where p is the maximal positive integer that makes the right term larger than the left one. In addition, the argument function $\arg(\cdot) \in [-\pi, \pi)$ by convention.

It can be noted from Fig. 8 that the Nyquist plot of the radial position delay-free loop gain crosses the unity circle at frequency $\omega_c = 59.682$ rad/sec with crossing point $(-0.928, -0.378)$. Therefore, $\|G(j\omega)\| = 1$ has only one root, and the stability condition is given by

$$-\pi + 59.682\tau < arg[G(j\ 59.682)] \Rightarrow \tau < 0.0064 \tag{13}$$

Similarly, the Nyquist plot of the plasma current delay-free loop gain crosses the unit circle at frequencies $\omega_{c1} = 1.61 \times 10^{-10}$ rad/sec and $\omega_{c2} = 5.3160$ rad/sec with crossing points $(0.00244, -1)$ and $(0.2989, -0.9543)$ respectively.

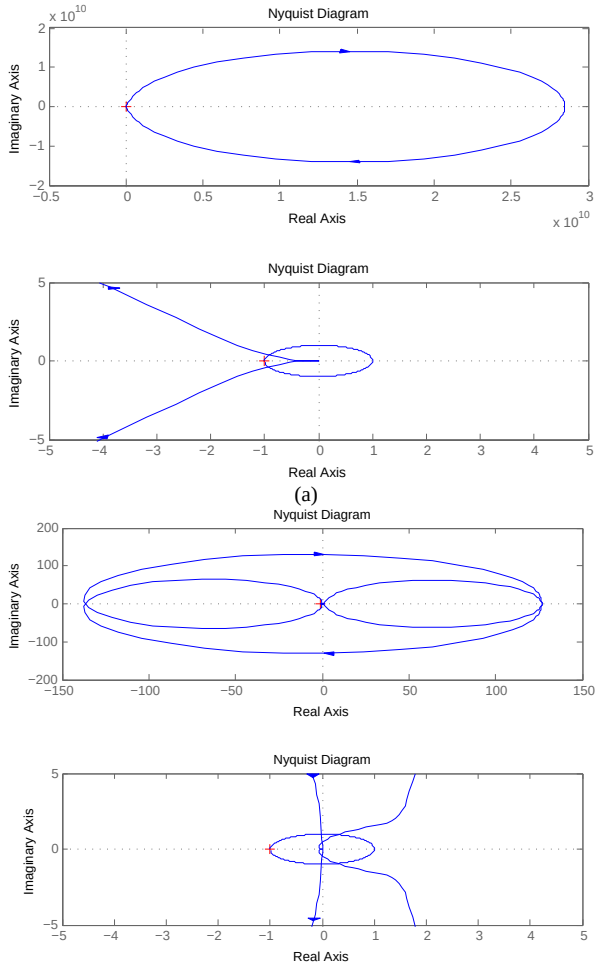

Fig. 8. Dual-locus: (a) R loop, (b) Ip loop. The bottom graph in each subfigure is a zoom of the top graph.

Therefore, $\|G(j\omega)\| = 1$ has two roots, and the stability condition is given by

$$-\pi + 5.3160\tau < arg[G(j\ 5.3160)] \Rightarrow \tau < 0.3525 \quad (14)$$

From the above stability conditions, it can be easily concluded that the whole system is stable if $\tau < 6.4$ ms.

The simulations in Fig. 9 show consistency with the obtained stability condition (the system is stable if $\tau < 6.4$ ms). The time delay is increased for the system controlled with the gains optimally tuned for $\tau = 1$ ms (see Fig. 7), which were used to obtain the stability condition. The closed-loop system is reaching the marginal stability condition for $\tau = 6$ ms and is already unstable for $\tau = 7$ ms.

It is important to emphasize at this point that the partial decoupling of the radial position and plasma current loops obtained through the ohmic-flux concept design allows to assess the stability of the whole system by studying independently the stability of the two control loops.

VII. Conclusions

In this work we reported on the effect of time delays on the closed-loop behavior of radial position and plasma current controllers in the superconducting KSTAR tokamak. Delays in the plasma control system, lags in the power supplies and delays produced by the resistance of the vessel were considered. The PID-based controllers were designed using the concept of ohmic flux, which guarantees in the ideal case that the regulation of the plasma current does not affect the plasma radial position.

Extremum seeking was introduced as an effective method for optimal tuning of the PID gains in the presence of time-delays. The simulation studies show that well-tuned PID controllers can successfully handle significant amounts of time delay. The dual-locus technique based on the Argument Principle in complex theory was employed to assess stability in the presence of time-delays of the overall closed-loop system controlled by the optimized PIDs.

In Section V we concluded that in terms of performance there is a practical limit of time delays that well-tuned PID controllers can handle. Beyond this limit an augmentation of the control loop is necessary. Our future work includes the design of robust predictors to handle larger values of time delays without deterioration of the tracking performance.

Acknowledgements

We gratefully acknowledge Dr. J. Y. Kim and Dr. Sang-hee Hahn of the National Fusion Research Institute of Korea for allowing us to use models and figures of the KSTAR Tokamak for this study.

References

[1] K. Kim *et al.*, "Status of the KSTAR superconducting magnet system development," *Nuclear Fusion*, vol. 45, pp. 783–789, 2005.
[2] K. Ariyur and M. Krstic, *Real-Time Optimization by Extremum Seeking Feedback*. Wiley, 2003.
[3] N. Killingsworth and M. Krstic, "PID tuning using extremum seeking," *IEEE Control Systems Magazine*, vol. 26, no. 1, pp. 70–79, 2006.
[4] M. Satche, "Discussion on stabilityof linear oscillating systems with constant time lag," *Journal of Applied Mechanics, Transactions of the ASME*, vol. 16, no. 4, p. 419420, 1949.
[5] O. J. M. Smith, *Feedback Control Systems*. New York: McGraw-Hill Book Company, Inc., 1958.
[6] L. L. Lao *et al.*, "Reconstruction of current profile parameters and plasma shapes in tokamaks," *Nuclear Fusion*, vol. 25, p. 1611, 1985.
[7] M. L. Walker and D. A. Humphreys, "Valid coordinate systems for linearized plasma shape response models in tokamaks," *Fusion Science and Technology*, vol. 50, pp. 473–489, 2006.
[8] D. A. Humphreys, J. A. Leuer, and M. L. Walker, "Minimal plasma response models for design of tokamak equilibrium controllers with high dynamic accuracy," *Bull. Am. Phys. Soc.*, vol. 44, pp. 175–182, 1999.
[9] M.L.Walker, "Calculation of feedforward current and voltage trajectories for shape and plasma current control," General Atomics," Engineering Physics Memo EPM060508a, 2006.
[10] J.-Y. Choi, M. Krstic, K. Ariyur, and J. Lee, "Extremum seeking control for discrete-time systems," *IEEE Transactions on Automatic Control*, vol. 47, no. 2, pp. 318–323, 2002.
[11] R. V. Churchill, *Complex Variables and Applications*. New York: McGraw-Hill Book Company, Inc., 1960.
[12] K. Gu, V. L. Kharitonov, and J. Chen, *Stability of Time-Delay Systems*. $Birkhäuser$, 2003.
[13] W. Michiels and S.-I. Niculescu, *Stability and Stabilization of Time-Delay Systems. An Eigenvalue-Based Approach*, ser. Advances in Design and Control. SIAM Publications, 2007, vol. 12.
[14] P. N. Nikiforuk and D. D. G. Nunweiler, "Dual-locus stability analysis," *International Journal of Control*, vol. 1, no. 2, p. 157166, 1965.
[15] L. Ou, W. Zhang, and D. Gu, "Nominal and robust stability regions of optimization-based PID controllers," *ISA Transactions*, vol. 45, no. 3, pp. 361–371, 2006.